



Shovelomics for phenotyping root architectural traits of rapeseed/canola (*Brassica napus* L.) and genome-wide association mapping

Muhammad Arifuzzaman¹ · Atena Oladzadabbasabadi¹ · Phillip McClean¹ · Mukhlesur Rahman¹

Received: 19 July 2018 / Accepted: 3 April 2019 / Published online: 9 April 2019
© Springer-Verlag GmbH Germany, part of Springer Nature 2019

Abstract

Root system in plants plays an important role in mining moisture and nutrients from the soil and is positively correlated to yield in many crops including rapeseed/canola (*Brassica napus* L.). Substantial phenotypic diversity in root architectural traits among the *B. napus* growth types leads to a scope of root system improvement in breeding populations. In this study, 216 diverse genotypes were phenotyped for five different root architectural traits following shovelomics approach in the field condition during 2015 and 2016. A single nucleotide polymorphism (SNP) marker panel consisting of 30,262 SNPs was used to conduct genome-wide association study to detect marker/trait association. A total of 31 significant marker loci were identified at 0.01 percentile tail *P* value cutoff for different root traits. Six marker loci for soil-level taproot diameter (R_1 Dia), six loci for belowground taproot diameter (R_2 Dia), seven loci for number of primary root branches (PRB), eight loci for root angle, and eight loci for root score (RS) were detected in this study. Several markers associated with root diameters R_1 Dia and R_2 Dia were also associated with PRB and RS. Significant phenotypic correlation between these traits was observed in both environments. Therefore, taproot diameter appears to be a major determinant of the canola root system architecture and can be used as proxy for other root traits. Fifteen candidate genes related to root traits and root development were detected within 100 kbp upstream and downstream of different significant markers. The identified markers associated with different root architectural traits can be considered for marker-assisted selection for root traits in canola in future.

Keywords GWAS · Shovelomics · Root architectural traits · *Brassica napus* · Marker assisted selection

Introduction

Brassica napus L. is an amphidiploid species (AACC) developed from natural hybridization of two other diploid *Brassica* species, *B. rapa* (AA) and *B. oleracea* (CC) (UN 1935). *B. napus* is one of the few *Brassica* species that are categorized as canola/rapeseed if its oil has less than 2% erucic acid and meal contains less than 30 μ m/gm glucosinolate. Rapeseed/canola oil is now regarded as one of the healthiest edible oils worldwide (Lin et al. 2013). It is the second

largest oilseed crop in terms of global production after soybean (Foreign Agriculture Services, USDA, 2017). *B. napus* canola includes three different growth types, spring, winter and semi-winter based on growing season and vernalization requirement for flowering (Ferreira et al. 1995; Rahman and McClean 2013). According to Kebede et al. (2010), the spring and winter canola are genetically diverse from one another. Besides their flowering time difference, spring and winter types are distinct in terms of other morphological characteristics. Winter type canola plants have larger leaves, wider stem diameters, higher plant height, and more vigorous root system with higher yield compared to spring canola (Rahman and McClean 2013; Arifuzzaman et al. 2016; Arifuzzaman and Rahman 2017). The phenotypic variation in root system between the canola growth types and genetic diversity among them provides a huge scope of identifying markers and/or loci controlling root system difference in canola.

The root system in plants has several major functions such as supplying water and nutrients, acting as food and

Communicated by S. Hohmann.

Electronic supplementary material The online version of this article (<https://doi.org/10.1007/s00438-019-01563-x>) contains supplementary material, which is available to authorized users.

✉ Mukhlesur Rahman
md.m.rahman@ndus.edu

¹ Departemnt of Plant Sciences, North Dakota State University, Fargo, ND, USA

water storage unit, and anchoring the plant to the soil (de Dorlodot et al. 2007). The spatial arrangement of the whole root system in the soil is referred to as its root system architecture (Lynch 2007). Different components of a root system, i.e., root length, primary root branch, lateral root branch, root density, root diameter, root angle, total root surface, etc. (Kuijken et al. 2015) define the root system architecture of that root system. Different root architectural traits respond to the soil microenvironment differentially and can be modified according to the plant needs. Therefore, the root system plays a significant role in adaptation of plants under abiotic stress conditions. According to Lynch (2007), greater focus should be implemented on the modification of root system to enhance crop adaptation under different environmental stresses to increase the crop production. Manipulation of root system architectural traits of crops to grow in nutrient deficient or drought condition can significantly enhance the yield (Wasson et al. 2012; Kuijken et al. 2015).

The root system has remained the “the hidden half” throughout the last century in the field of plant breeding and crop improvement. Plasticity of the root system and difficulties in phenotyping root traits has discouraged breeder from focusing on root traits for crop improvement. Recent advancement in genetic mapping and molecular marker technologies encouraged breeders to emphasize on the root architectural traits for crop improvement through marker assisted selection (Clark et al. 2011). Nevertheless, large-scale, highly accurate and efficient phenotyping of root traits is essential for an ideal mapping study (Canè et al. 2014). Recent technological advances in the field of phenomics allow plant breeders to successfully evaluate the root architecture of different crops from younger seedlings in controlled environment. There are very few methods for large-scale high-throughput phenotyping for the root architectural traits in the field. Shovelomics is one of the popular methods of root system phenotyping in the field. Shovelomics involves digging up the root system with shovel from the field, washing them and measuring the root traits with the help of a phenotyping board and/or imaging technology (Trachsel et al. 2011).

Genome-wide associate studies (GWAS) were first implemented to study human diseases as an alternate to family based mapping strategies (Begum et al. 2015). Eventually, it becomes very popular among plant scientists to identify quantitative trait loci. A GWAS is performed with a set of diverse genotypes which enable us to capture all the historical recombination events within a germplasm panel (Zhao et al. 2014; Rahaman et al. 2017) and is highly efficient in identifying common alleles controlling a complex trait. Single nucleotide polymorphism (SNP) markers are now the most popular marker due to their low cost and ease of development. Researchers are now able to develop genetic

maps with higher marker density with the help of abundantly generated SNPs (Luo et al. 2016).

Genome-wide association mapping is performed to successfully identify QTL and molecular markers associated with different root traits in different crops. However, most of these studies were performed under controlled condition. There are only few examples of phenotyping for root architectural traits in the field; i.e., rice with PVC pipe method (Li et al. 2017), rice with basket method (Lou et al. 2015), and cowpea with shovelomics (Burridge et al. 2017) to use in genome-wide association mapping studies. In the current study, we adopted the shovelomics approach described by (Trachsel et al. 2011) to phenotype genetically diverse *B. napus* germplasms for different root architectural traits, and to identify genomic regions associated with different root architectural traits of rapeseed/canola (*B. napus* L.)

Materials and methods

Plant materials and experimental design

A total of 216 *B. napus* genotypes of diversified origin (Supplementary Table 1) were planted in North Dakota State University Agricultural Experiment Station at Carrington, N. D. in mid May of 2015 (47.516998, – 99.148217) and mid May of 2016 (47.517740, – 99.144523). The soil type of the area is Heimdahl silt loam with pH of ~6.5 and OM of ~2.7. Each genotype was grown in a single row plot with 3 cm plant spacing and 61 cm row spacing. All the three growth habit types of canola/rapeseed were included in the germplasm panel: spring ($n=85$), winter ($n=90$) and semi-winter ($n=39$), rutabaga ($n=2$) and grown in the same field within a year to maintain the uniformity of the growing condition. The germplasm accessions were obtained from Germplasm Resource Information Network (GRIN) of USDA-ARS. Germplasms were planted as randomized complete block design with two replications in each year.

Phenotyping

Root architectural traits were phenotyped with the shovelomics approach described by (Trachsel et al. 2011). Phenotyping was done at 50 days after planting. The total phenotyping procedure is divided into three major steps (Fig. 1). Three representative plants per plot were selected based on plant height and general appearance and excavated them with a shovel. The root system in 50-day-old canola plant is very complex and grows deep in the soil horizon. Therefore, we excavated the root system only to capture the top 10 cm of the root system and phenotyped the root traits. The root sample is then washed. All three excavated plants with their root systems were zip tied together, tagged and

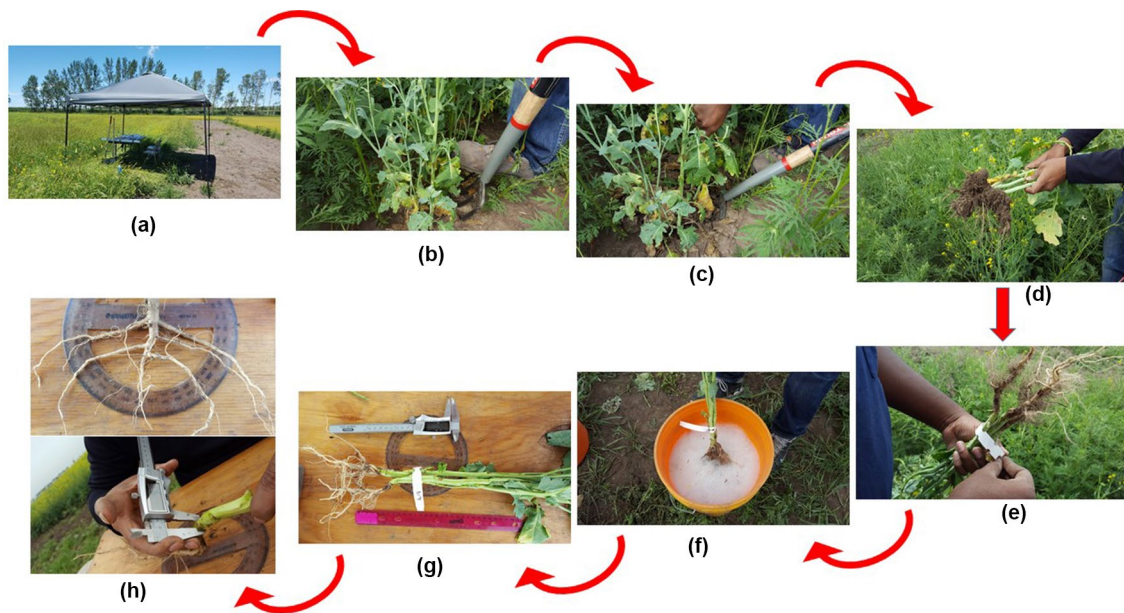


Fig. 1 Shovelomics in phenotyping root system architectural traits of canola. **a** Work station in the field, **b** selecting representative plants and excavating, **c** excavating, **d** clearing dirt, **e** tagging, **f** washing, **g** phenotyping board, **h** data collection

brought to the washing area. The roots were washed first with soapy water followed by a wash with normal water. After 5–10 min of air drying, data measurements were taken. Data were collected on the number of primary root branches (PRB), lateral root angle (RA), taproot diameter at soil level (R_1 Dia), belowground taproot diameter at 10 cm below the soil level (R_2 Dia) and a visual scoring of the root system (RS) (Table 1). RA and the first 10 cm length of the taproot were measured with a phenotyping board labeled with angle and length measurement. Diameters were taken with slide calipers at the soil surface position and 10 cm down from the first data point. RS was recorded with a visual scoring system based on general appearance of the root system and scored from 1 to 5, where score “1” represents the weakest root system with the thinnest taproot and fewest branch roots, score “2” represents weak root system with thin taproot and less root branches, score “3” represents root system with intermediate taproot diameter and intermediate root branches, score “4” represents root system with higher root

vigor, thick taproot and root branches and score “5” represents very vigorous root system with the thickest taproot and higher number of root branches (Fig. 2).

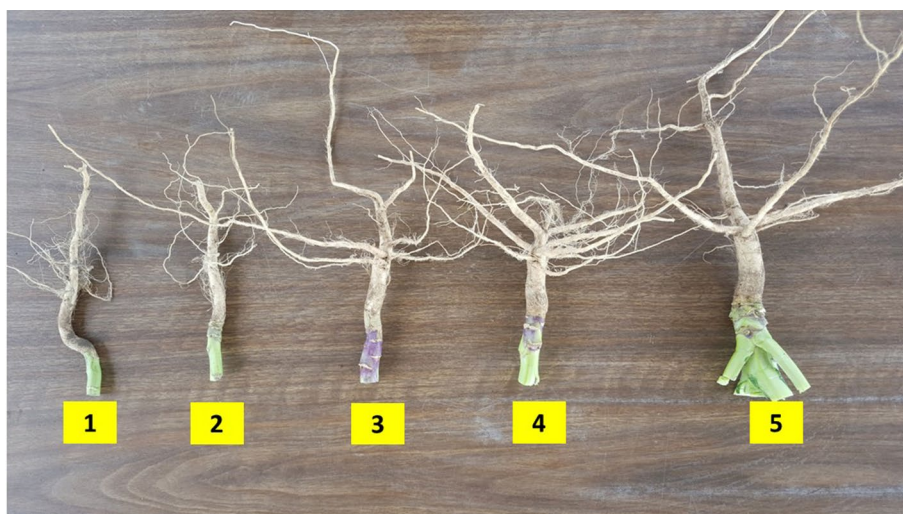
Statistical analysis

Data from three representative plants per plot were averaged and were analyzed 2015 (E1) and 2016 (E2) separately in SAS 9.3 (SAS Institute Inc., USA). Means were used to construct the analysis of variance (ANOVA) for all traits except RS, for which the medians were calculated and used. If the ratio of the effective error variance for each trait is less than tenfold, data from both environments were combined and used for the GWAS analysis (Tabachnick and Fidel 2001; Elias and Manthey 2016). Pearson correlation coefficients were calculated in SAS 9.3 for all traits except RS for which spearman correlation coefficient was calculated. Shapiro–Wilk test was conducted in SAS 9.3 for all traits in both E1 and E2 and combined dataset. Entry mean basis

Table 1 Root architectural traits, their abbreviation and description used in this study

Trait	Abbreviation used	Description
Soil level taproot diameter	R_1 Dia	Taproot diameter at the soil level
Belowground taproot diameter	R_2 Dia	Taproot diameter at 10 cm below the soil level
Primary root branch number	PRB	Number of primary root branches came out from the taproot at top 10 cm of the root system
Root angle	RA	Angle between the two top most primary root branches came out from the taproot
Root scoring	RS	Visual scoring of the root excavated root system

Fig. 2 Visual root scoring with 1–5 scale, where (1) is the weakest root system with low taproot diameter and primary root branches and (5) is the strongest root system with high taproot diameter



heritability was calculated in SAS 9.3 for all traits in both E1, E2, and combined dataset. RS data were available for only one replication in E1 and, therefore, the heritability was not calculated for RS in E1.

Genotyping

A total of 366 germplasms from diverse origin and sources were planted in the greenhouse in 2013 (Michalack et al., Unpublished). Young leaf tissues were collected from each germplasm and freeze dried. DNA was extracted using Qiagen DNeasy kit (Qiagen, CA, US) following the manufacturer's protocol. After extraction, DNA was quantified, checked for quality, optimized and sent to Institute of Genomic Diversity (IGD), Cornell University for Genotyping by Sequencing (GBS). GBS libraries were prepared using *ApeKI* single cutter enzyme following the protocol described by (Elshire et al. 2011). Libraries were sequenced with Illumina GAI sequencer, and 100 bp single end sequenced GBS data were aligned using BWA-MEM (Li 2013). VarScan (Koboldt et al. 2012) was used for SNP calling. SNPs were imputed for missing allele using FastPHASE (Scheet and Stephens 2006) and finally 42,575 SNPs were obtained. For the current experiment, we used the SNP data with minor allele frequency greater than 0.05 on 216 genotypes. The name of each SNP marker consists of chromosome number and physical position of that marker. For example, an SNP marker located on 123456 bp of chromosome C04 was named as "C04_123456".

Marker-trait association

Association mapping was performed using GAPIT R-based program (Lipka et al. 2012). A number of principle components (PC) that collectively explain 25% of the variation in the population were determined by principle component

analysis (PCA) in R 3.4.1 using *prcomp* () function (Price et al. 2006). A pairwise kinship coefficient matrix was calculated to account for individual relatedness using the EMMA algorithm (Kang et al. 2008) embedded in GAPIT. A total of four models were tested to detect the marker-trait association: (1) a null general linear model or naïve model accounting for neither population structure nor kinship (EMMA); (2) a general linear model accounting for population structure as a fixed effect using the number of PC accounting for 25% of the variation (PC-25%); (3) an efficient mixed model association or EMMA accounting for kinship in the population; and (4) a mixed linear model accounting for both population structure and kinship, PC-25% + EMMA. All the models were compared on a rank-based mean square difference (MSD) value, and the model with the lowest MSD value was selected as the best model (Mamidi et al. 2011). Significant markers were declared based on the *P* value of the markers at lower 0.01 and 0.1 percentile tail of an empirical distribution obtained by 10,000 bootstraps (Mamidi et al. 2014). Manhattan plots were created using *mhtplot* () function in R statistical software package gap (Zhao 2007). Log likelihood ratio-based R^2 or R^2_{LR} (Sun et al. 2010) was calculated in genAble package in R.4.1 (Aulchenko et al. 2007) for the most significant markers in the best models to determine the phenotypic variation explained by those markers.

Candidate gene

B. napus gene models within 100 kbp upstream and downstream of the significant markers were taken into account for candidate gene search. Protein sequences from the gene models were blasted against TAIR 10 protein database to determine the gene annotation. Genes associated with root development were identified based on the Gene Ontology terms (GO terms) from TAIR website and gene functions found in previous literatures.

Results

Phenotypic distribution

Phenotypic variation was observed among the germplasm panel in both environments and when the data were combined (Fig. 3). The range between maximum and minimum observations in 2015 for R₁Dia (22.88), R₂Dia (8.15), PRB (13.80) and RA (96.79) was higher than that of 2016 (Table 2). The CVs of R₁Dia (27%), R₂Dia (44%), PRB

(31%) and RS (31%) in 2015 were higher than the CVs for the respective traits in 2016. Relatively higher CV was observed for R₂Dia across both environments and the combined dataset (31–44%). The lowest CVs were observed for RA across both years and with the combined datasets ranging 6–9%. High family based mean heritability was detected for R₁Dia in both years and for combined dataset (0.60–0.79) (Table 2). High heritability was detected for R₁Dia in 2015 (0.83), but moderate heritability was detected in 2016 (0.60) and the combined dataset (0.67). A similar trend of high heritability in 2015 (0.72) and

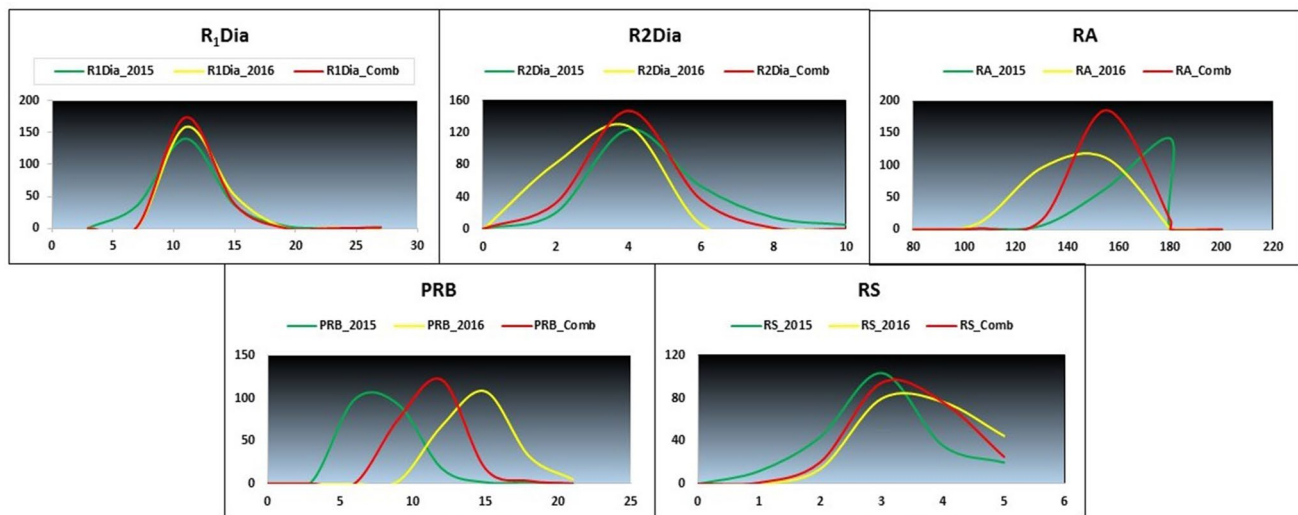


Fig. 3 Phenotypic distribution of different root architectural traits in 2015, 2016 and combined dataset

Table 2 Phenotypic variation in different root architectural traits

Traits	Env.	Unit	Mean (\pm std)	Range	CV (%)	Shapiro–Wilk test p value	h^2 (family mean basis)
R ₁ Dia	2015	mm	9.35 (\pm 2.57)	22.88	27	0.0001	0.79
	2016	mm	10.08 (\pm 1.84)	13.34	18	0.0001	0.60
	Comb	mm	9.71 (\pm 1.92)	17.27	19	0.0001	0.67
R ₂ Dia	2015	mm	3.61 (\pm 1.61)	8.15	44	0.0001	0.83
	2016	mm	2.28 (\pm 0.71)	4.45	31	0.0001	0.32
	Comb	mm	2.95 (\pm 0.98)	4.86	33	0.0001	0.41
PRB	2015	Number	6.49 (\pm 2.07)	13.80	31	0.0001	0.72
	2016	Number	13.09 (\pm 2.15)	11.70	16	0.0378	0.56
	Comb	Number	9.79 (\pm 1.64)	11.2	17	0.0001	0.39
RA	2015	Degree	157.18 (\pm 13.31)	96.79	8	0.0001	0.43
	2016	Degree	128.70 (\pm 11.36)	63.75	9	0.0001	0.60
	Comb	Degree	142.94 (\pm 9.08)	56.53	6	0.0001	0.33
RS	2015	Scoring	2.95 (\pm 0.93)	4.00	31	0.0001	NA
	2016	Scoring	3.47 (\pm 0.87)	3.75	25	0.0001	0.58
	Comb	Scoring	3.33 (\pm 0.78)	4.00	23	0.0001	0.46

Note: NA = not available

moderate heritability in 2016 (0.56) and the combined dataset (0.39) was found for PRB. Very low heritability was observed for RA in combined dataset (0.33). RS heritability in 2015 and combined dataset found moderate ranging from 0.46 to 0.58.

Correlation among the traits

A significant positive correlation ($r=0.57-0.65$, $P<0.001$) was detected between R_1 Dia and R_2 Dia in all datasets (Fig. 4). Both the root diameters, R_1 Dia and R_2 Dia, were significantly ($P<0.001$) positively correlated with RS in all datasets. PRB and R_1 Dia were also significantly ($P<0.001$) correlated with each other in all environment. Very low or negative nonsignificant correlation was detected between RA and all other traits.

Genotypic data and principle component analysis

Originally 366 genotypes were genotyped from which 42,575 single nucleotide polymorphism (SNP) markers were obtained as described by Michalack et al. (Unpublished). In this current study, a subset of 216 genotypes was used. From the original panel, 30,262 markers were retained for the panel evaluated here after correcting for $MAF>5\%$ and were used finally in this current study. Principle component analysis was performed to control for population structure. The first two principle components grouped the population into three continuous sub-populations (Fig. 5). The first three principle components accounted for 25% of the population variation and were included in the association analysis as general linear model.

Fig. 4 Correlation among the root architectural traits in 2015, 2016 and combined dataset

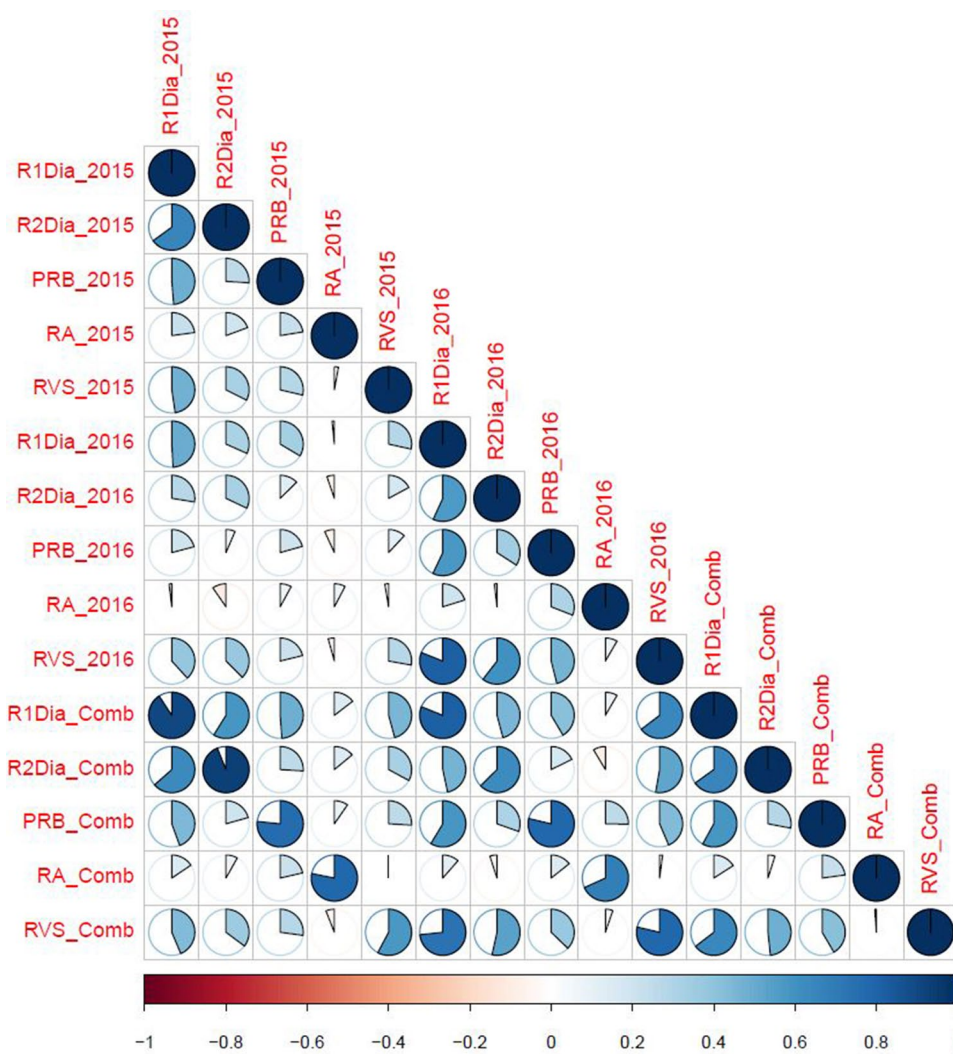
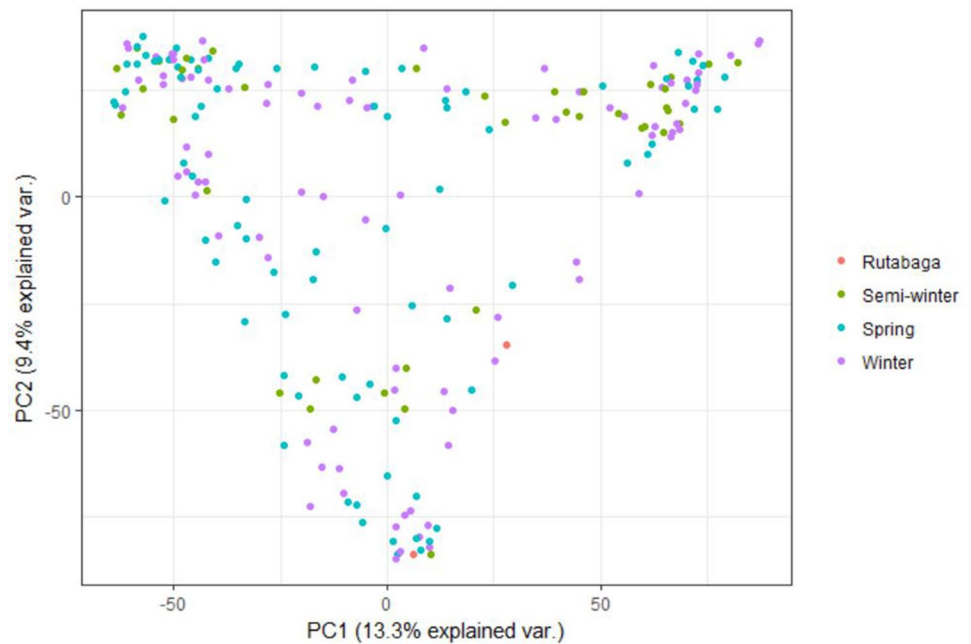


Fig. 5 Principle component graphs showing the distribution of the population used in this study



Marker-trait association

Four models were tested for each trait in each year and with the combined over the two years to detect best SNP marker/trait association. Among the models, the best model was selected based on the lowest MSD value (Mamidi et al. 2014; Soltani et al. 2017). The P values of the best model for a trait in a particular dataset (2015, 2016 or combined) were bootstrapped 1000 times, and the P value at 0.01 percentile of the empirical distribution was set as the cutoff for that particular trait in the respective dataset. Highly stringent P value cutoff increases the chance of eliminating false positive or the false association. However, it also increases the chance of excluding false negative or true association. To reduce the chance of excluding true association or falls negative, we fixed another less stringent P value cutoff at 0.1 percentile of the empirical distribution (Moghaddam et al. 2016). Only the markers that were found to be appear repeatedly for a trait in both years and the combined dataset were considered to be a significant association and were reported here. Candidate genes were searched 100 kbp at either side of a significant marker at 0.01 percentile cutoff.

Soil level taproot diameter (R_1 Dia)

The mixed linear model accounting for relatedness in the population was the best fitted model in both years and combined over the 2 years (Supplementary Table 2). Three markers, chrA01_rand_2039614, chrC01_rand_171065, and chrC04_4933647, were found to be associated with R_1 Dia in 2015 at the 0.01 percentile P value cutoff level (Table 3). The markers together explained 39.2% of the

phenotypic variation. Marker locus chrA01_rand_2039614 from 2015 was also detected in 2016 and the combined dataset. Marker locus chrC01_rand_171065 from 2015 was also detected in combined dataset. In 2016, two other markers chrC02_30907736 and chrA09_32034416 explaining 16.2%, and 16.8% of the phenotypic variation, respectively, were detected. Two root-related candidate genes, *STRUB-BELIG-receptor family 3 (SUB)*, were detected nearby the marker locus chrA09_32034416 (2016). Marker chrC05_rand_678307 was detected in combined dataset and two candidate genes, *Cyclin-dependent kinase 2;3 (CYC2; 3)* and *P-glycoprotein 11 (PGP 11)*, were detected nearby physical location of the marker.

Bottom taproot diameter (R_2 Dia)

A general linear model using the first three principal components was selected as the best model for R_2 Dia in 2015 and combined data (Supplementary Table 2). Three markers loci, chrA08_18428869, chrA08_18428839 and chrA08_18441370, within a very close physical distances on chromosome A08 were identified as the significant markers at 0.01 percentile P value cutoff in both 2015 and the combined dataset (Table 3). The markers altogether explained 13.2% and 9.8% of the phenotypic variation in 2015 and combined dataset, respectively. The fact that the three loci only marginally account for more of the phenotypic variation suggests that they are linked to the same causative locus. Two candidate genes, *AUXIN RESISTANT 3 (AXR3)* and *Cryptochrome 2 (CRY2)*, were identified in the same region of chromosome A08 (Table 4). A mixed linear model, PC3 + EMMA, accounting for both population structure and

Table 3 Significant markers for different root architectural traits in 2015, 2016 and combined datasets at 0.01 percentile

Trait	Markers	Year (0.01)	Year (0.1)	Allele	MAF	−log ₁₀ (<i>P</i> -value)	<i>R</i> ² (%)
R ₁ Dia	chrA01_rand_2039614	2015, 2016, Comb		C/T	0.14	4.76	18.49
	chrC01_rand_171065	2015, Comb		G/C	0.05	4.64	17.86
	chrC04_4933647	2015, Comb		A/T	0.11	3.58	13.36
						Total	39.24
	chrA01_rand_2039614	2016, 2015, Comb		C/T	0.14	4.37	11.65
	chrC02_30907736	2016	Comb	A/G	0.13	4.35	16.21
	chrA09_32034416	2016		A/T	0.16	4.30	16.79
						Total	31.99
	chrA01_rand_2039614	Comb, 2015, 2016		C/T	0.14	5.81	22.93
	chrC01_rand_171065	Comb, 2015		G/C	0.05	4.49	17.79
	chrC05_rand_678307	Comb	2015, 2016	C/T	0.26	3.99	14.45
						Total	45.43
R ₂ Dia	chrA08_18428869	2015, Comb		T/C	0.20	5.99	12.25
	chrA08_18428839	2015, Comb		A/G	0.20	5.75	11.54
	chrA08_18441370	2015, Comb		G/T	0.21	5.25	10.36
						Total	13.15
	chrC05_7043010	2016		T/A	0.15	3.80	14.82
	chrA10_5618818	2016		C/T	0.48	3.57	15.76
	chrA09_6247199	2016		G/A	0.07	3.44	13.56
						Total	33.78
	chrA08_18428869	Comb, 2015		T/C	0.20	4.63	9.27
	chrA08_18428839	Comb, 2015		A/G	0.20	4.49	8.78
	chrA08_18441370	Comb, 2015		G/T	0.21	4.12	7.91
						Total	9.76
PRB	chrC01_rand_171065	2015, Comb		G/C	0.05	5.25	18.04
	chrC04_24065408	2015	Comb	T/A	0.12	3.98	18.00
	chrC03_3328679	2015		A/T	0.18	3.79	17.31
						Total	37.37
	chrC05_7907786	2016		T/C	0.36	4.27	8.20
	chrA08_6097421	2016		A/T	0.45	3.93	10.45
						Total	16.90
	chrA06_2653673	Comb	2015, 2016	C/T	0.13	4.59	9.15
	chrC01_rand_171065	Comb, 2015		G/C	0.05	4.04	8.30
	chrA08_4600588	Comb	2015	C/A	0.09	3.85	7.56
						Total	22.45
	RA	chrA02_18466347	2015, Comb		A/G	0.49	4.17
chrA09_8677526		2015		G/A	0.13	4.16	7.29
chrA03_25132124		2015		G/C	0.13	3.79	6.49
						Total	21.09
chrC03_36049749		2016		C/T	0.35	2.88	10.90
chrA03_18531995		2016		A/C	0.10	2.86	10.30
chrC09_8316001		2016		T/A	0.132	2.83	9.12
						Total	29.75
chrA02_18466347		Comb, 2015		A/G	0.49	4.75	16.23
chrC06_35857438		Comb		C/T	0.06	3.94	16.23
chrA02_22847077		Comb		G/A	0.09	3.87	12.83
						Total	32.85
RS	chrC01_11345932	2015		C/T	0.22	4.89	17.34
	chrC09_19217839	2015		C/T	0.43	3.53	13.05
	chrC05_13423686	2015		G/A	0.24	3.41	12.08

Table 3 (continued)

Trait	Markers	Year (0.01)	Year (0.1)	Allele	MAF	−log ₁₀ (<i>P</i> -value)	<i>R</i> ² (%)
						Total	28.48
	chrC09_23510860	2016		C/T	0.15	3.46	5.84
	chrA01_rand_2039614	2016, Comb		C/T	0.14	3.43	5.78
	chrC05_rand_678307	2016	Comb	C/T	0.26	3.36	5.63
						Total	17.25
	chrA09_32034416	Comb		A/T	0.16	3.84	14.53
	chrA09_32034411	Comb	2016	A/T	0.16	3.39	12.64
	chrA01_rand_2039614	Comb, 2016		C/T	0.14	3.07	10.66
						Total	20.46

relatedness was selected as the best model in 2016. Three unique marker loci, chrC05_7043010, chrA10_5618818 and chrA09_6247199, were found to be significantly associated with *R*₂Dia in 2016. They altogether accounted for 33.8% of the phenotypic variation (Table 3).

Primary root branches (PRB)

EMMA, accounting for kinship in the population, was found to be the best model for PRB in 2015 (Supplementary Table 2). On the other hand, PC3, accounting for population structure, was identified as the best fitted model in 2016 and combined dataset. In 2015, marker loci, chrC01_rand_171065, chrC04_24065408 and chrC03_3328679, were identified as the significant markers associated with PRB at 0.01 percentile *P* value cutoff and accounts for 37.4% of the phenotypic variation (Table 3). *GAST1*, a homolog of *GASA4*, was detected at 53 kbp upstream of the marker locus chrC03_3328679 (Table 4). One of the 2015 marker loci, chrC01_rand_171065, was also detected in combined dataset and explained 9.2% phenotypic variation. Two other unique markers, chrA06_2653673 and chrA08_4600588, were also found to be significantly associated with PRB in combined dataset. Marker locus chrA06_2653673 was also found to be associated with PRB in both E1 and E2 with a less stringent at 0.1 percentile *P* value cutoff. A lateral organ boundaries (LOB) domain family (LBD1) gene was detected at 30 kbp upstream of the marker locus chrA06_2653673. At 0.01 percentile *P* value cutoff, two markers, chrC05_7907786 and chrA08_6097421, were identified in 2016 and explained 16.9% of the phenotypic variation. *Aminotransferase-like, plant mobile domain family protein (MAIN)* was detected at 87 kbp downstream of the marker locus chrC05_7907786.

Root angle (RA)

The naïve model, accounting for neither the population structure nor kinship, was the best model in 2015 for RA (Supplementary Table 2). A mixed linear model including kinship

and PC3+EMMA was the best model in 2016 and combined dataset, respectively. Marker locus, chrA02_18466347, was detected as the most significant marker associated with root angle in both 2015 and combined dataset (Table 3). This marker explained 7.3% and 16.2% of the total phenotypic variation in 2015 and combined dataset, respectively. The other two marker loci found to be significantly associated with RA in 2015 are chrA09_8677526 and chrA03_25132124 and accounted 7.3% and 6.5% of the total phenotypic variation, respectively. Candidate gene *SABRE*-like protein (*SABRE*) and auxin-responsive *GH3* family were detected at 58 kbp upstream and 34 kbp downstream, respectively, of the marker locus chrA09_8677526 (Table 4). Candidate genes, *Cytokinin response factor 4 (CRF4)* and *Tetraspanin 7 (TET7)*, were detected at 5 kbp and 36 kbp downstream, respectively, of the marker locus chrA03_25132124. Three marker loci, chrC03_36049749, chrA03_18531995 and chrC09_8316001, were detected for RA in 2016, and they altogether explained 29.8% of the total phenotypic variation. Two unique marker loci, chrC06_35857438 and chrA02_22847077, were detected in combined dataset. *Auxin-responsive factor 17 (ARF17)* was detected at 99 kbp downstream of the marker locus chrC06_35857438 associated with RA in combined dataset. Another candidate *GA requiring 3 (GA3)* was detected at 36 kbp downstream of the marker chrA02_22847077 associated with RA in combined dataset.

Root score (RS)

A mixed linear model including kinship was found to be the best model in 2015 and the combined analysis (Supplementary Table 2). Three marker loci, chrC01_11345932, chrC09_19217839 and chrC05_13423686, were found to be significantly associated with RS in 2015 at 0.01 *P* value cutoff (Table 3). The markers together explained 28.5% of the total phenotypic variation. Candidate gene *Cytokinin responsive factor 6 (CRF6)* was detected at 89 kbp upstream of the marker locus chrC09_19217839 (Table 4). In combined

Table 4 Candidate genes for different root architectural traits within 100 kbp region at either side of the significant markers

Trait	Locus	BNA gene model	AT match	Distance (Kbp)*	Name (TAIR)	Symbol (TAIR)	GO biological process (TAIR)
R ₁ Dia	chrA09_32034416	BnaA09g47730D	AT1G11130	– 91.7	<i>STRUBBELIG-receptor family 3</i>	<i>SUB, SCM, SCRAMBLED</i>	Root meristem specification
	chrC05_rand_678307	BnaC05g49810D	AT1G15570	80.3	<i>Cyclin-dependent kinase 2;3</i>	<i>CYCA2;3, CYCLIN A2;3</i>	Lateral root formation
		BnaC05g01280D	AT1G02520	9.9	<i>ABC transporter family, P-glycoprotein 11</i>	<i>PGP 11</i>	Auxin efflux transmembrane transporter activity; basipetal auxin transport
R ₂ Dia	chrA08_18428869	BnaA08g27770D	AT1G04250	18.5	<i>AUXIN RESISTANT 3</i>	<i>AXR3, IAA17</i>	Auxin-activated signaling pathway, response to auxin
	chrA08_18441370	BnaA08g27870D	AT1G04400	1.9	<i>Cryptochrome 2</i>	<i>CRY2</i>	Root development
PRB	chrC03_3328679	BnaC03g06850D	AT5G15230	53.9	<i>GAST1 protein homolog 4</i>	<i>GASA4</i>	Response to gibberellin stimulus, gibberellic acid mediated signaling pathway
	chrC05_7907786	BnaC05g13870D	AT1G17930	– 87.7	<i>Aminotransferase-like, plant mobile domain family protein</i>	<i>MAIN, MAINTENANCE OF MERISTEMS</i>	Meristem development
	chrA06_2653673	BnaA06g04390D	AT1G07900	30.7	<i>Lateral organ boundaries (LOB) domain family</i>	<i>LBD1</i>	Organ boundary specification, lateral root formation
RA	chrA09_8677526	BnaA09g14910D	AT1G58250	58.4	<i>SABRE-like protein, HYPERSENSITIVE TO PI STARVATION 4</i>	<i>HSP4, SABRE</i>	Negative regulation of ethylene-activated signaling pathway, response to ethylene
		BnaA09g15010D	AT1G48670	– 34.2	<i>Auxin-responsive GH3 family</i>	<i>Auxin-responsive GH3 family</i>	Response to auxin
	chrA03_25132124	BnaA03g48910D	AT4G27950	– 5.2	<i>Cytokinin response factor 4</i>	<i>CRF4</i>	Cytokinin-activated signaling pathway, ethylene-activated signaling pathway
		BnaA03g48970D	AT4G28050	– 36.8	<i>Tetraspanin 7</i>	<i>TET7</i>	Aging, root and leaf radial pattern formation, root morphogenesis
	chrC06_35857438	BnaC06g38360D	AT1G77850	– 99.5	<i>Auxin-responsive factor 17</i>	<i>ARF17</i>	Auxin-activated signaling pathway
chrA02_22847077	BnaA02g31830D	AT5G25900	– 67.4	<i>GA requiring 3</i>	<i>GA3</i>	Gibberellic acid mediated signaling pathway, gibberellin biosynthetic process	
RS	chrC09_19217839	BnaC09g21990D	AT3G61630	89.6	<i>Cytokinin response factor 6</i>	<i>CRF6</i>	Cytokinin-activated signaling pathway, ethylene-activated signaling pathway
	chrC05_rand_678307	BnaC05g49810D	AT1G15570	80.3	<i>Cyclin-dependent kinase 2;3</i>	<i>CYCA2;3, CYCLIN A2;3</i>	Lateral root formation

Table 4 (continued)

Trait	Locus	BNA gene model	AT match	Distance (Kbp)*	Name (TAIR)	Symbol (TAIR)	GO biological process (TAIR)
		BnaC05g01280D	AT1G02520	9.9	<i>ABC</i> transporter family, <i>P-glycoprotein 11</i>	<i>PGP 11</i>	Auxin efflux transmembrane transporter activity; basipetal auxin transport
	chrA09_32034416	BnaA09g47730D	AT1G11130	− 91.7	<i>STRUBBELIG-receptor family 3</i>	<i>SUB, SCM, SCRAMBLED</i>	Root meristem specification

*Negative values = genes are downstream of the marker, positive values = genes are upstream of the marker

dataset, three additional marker loci, chrA09_32034416, chrA09_32034411 and chrA01_rand_2039614, explained 20.4% of the total phenotypic variation were detected. A candidate gene *STRUBBELIG-receptor family 3 (SUB)* was located on chromosome A09, close to the marker loci chrA09_32034416 and chrA09_32034411. Marker locus chrA01_rand_2039614 was also appeared in 2016 and explains 5.8% of the total phenotypic variation. Two other marker loci, chrC09_23510860 and chrC05_rand_678307, were also detected in 2016, and explained 5.8% and 5.6% of the total phenotypic variation, respectively. Candidate gene, *P-glycoprotein 11 (PGP 11)*, was detected only 10 kbp upstream of the marker locus chrC05_rand_678307. Naïve model was selected as the best fitted model for 2016 based on the lowest MSD value.

Discussion

Shovelomics in *B. napus*

Plant breeders have historically modified the above ground morphological plant architecture of a crop to improve productivity. One of the greatest examples is the green revolution that developed high yielding dwarf varieties in wheat (Vergauwen and De Smet 2017). Modifying shoot features like branch angle and leaf angle are also regarded as the potential to improve the productivity of corn (Gong et al. 2015) and sorghum (Truong et al. 2015). This enabled increasing planting density, the capture of more sunlight, and increased photosynthetic efficiency of the crops. Similarly, the below ground root architectural traits can also be used as a target for improvement and optimization according to the necessities based on soil environment. Several studies on crops such as rice (Courtois et al. 2013), wheat (Canè et al. 2014), maize (Pace et al. 2015), cowpea (Burrige et al. 2017), and rapeseed (Wang et al. 2017) phenotyped the root system and mapped associated loci using GWAS for root architectural traits. Thomas et al. (2016) characterized the root morphology of different *B. napus* growth

types with “pouch and wick system” and concluded that root morphology can potentially be used to improve crop yield if suitable markers loci corresponding to agronomic traits can be identified.

The majority of these studies adopted root system phenotyping strategy that is feasible for controlled environment using soil or other growing media and phenotyped the root system of young seedlings. The root systems of young seedlings grown in hydroponics or soil in the controlled environment may not be indicative of the architecture that forms in the actual field condition (Zhu et al. 2011). Several researchers mentioned the importance of monitoring root architectural traits over the whole growth period in the soil condition as the root system architecture changes greatly over time (Hund 2010; Kumar et al. 2012; Passioura 2012; Colombi et al. 2015). Therefore, phenotyping the root system under all stages of growth in the field condition is immensely important, and high-throughput phenotypic techniques should be developed to overcome the difficulties in exploring root system in the field.

Unfortunately, very few high-throughput platforms for phenotyping the root system architecture in the field have been developed to date. Shovelomics is a high-throughput root phenotyping system first described by Trachsel et al. (2011). However, only a few studies have adopted this shovelomics approach to characterize the root system in field conditions in different crops. This includes crops such as maize (Bucksch et al. 2014; Colombi et al. 2015; York and Lynch 2015), in common bean and cowpea (Burrige et al. 2016). Although Trachsel et al. (2011) proposed manual measurement of the data in the original shovelomics approach, most studies used image-based technologies during data collection. Burrige et al. (2017) conducted a GWAS analysis for cowpea root architectural traits with the phenotypic data collected with shovelomics approach. In the current study, we also adopted the field-based shovelomics technique to phenotype 216 *B. napus* genotypes in multiple years and used that data for a GWAS analysis. This is the first report of shovelomics to characterize the root architectural traits in *B. napus*.

In the current study, we have phenotyped five root traits and conducted a GWAS analysis. Based on a stringent cutoff at lower 0.01 percentile of bootstrap *P* values, 31 marker loci were associated with different root traits in 2015, 2016 and in the combined datasets. Markers were distributed in all the *B. napus* chromosomes except A04, A05, A07, C07 and C08. Five marker loci were detected on chromosome A08 controlling R_2 Dia and PRB. Four marker loci controlling various root traits were detected on chromosome A09. Multiple co-localized marker loci were detected on chromosome A08 and A09 controlling primary root number under high and low P level (Zhang et al. 2016).

Phenotypic distribution and correlation among the root architectural traits

In the current study, five different root architectural traits R_1 Dia, R_2 Dia PRB, RA and RS in 2015 and 2016 were phenotyped. Analysis was performed for both years and the combined dataset. Population means were relatively constant across the years for R_1 Dia, R_2 Dia and RS. In contrast, population means for PRB and RA varied across years indicating a genotype \times environment effect controlling these traits. Development of lateral root branches is highly responsive to the soil nitrogen (N) and phosphorus (P) condition and water regime. On the basis of range, phenotypic variation within the population was always higher in 2015 to 2016. This also indicates the environmental influences controlling the root traits. Entry mean basis heritability for different traits varied with environments. High heritability values were noted for R_1 Dia, R_2 Dia and PRB in 2015. However, the heritability values decreased to moderate levels for all these traits in 2016 suggesting high environmental variation between these two environments.

Significant and high correlation was observed among the traits within the same year and in the combined datasets. R_1 Dia and R_2 Dia are highly correlated in both environment and combined datasets. A high correlation was also observed between PRB and R_1 Dia. This is expected as the taproot having high diameter will have more surface area to grow more primary and lateral root branches and the root will be more vigorous. This statement is supported further as a high positive correlation was observed between R_1 Dia and RS and between PRB and RS. Visual root scoring was conducted based on the overall appearance of the root system on top soil considering diameter and root branches. Low but significant positive correlation was detected between R_2 Dia and PRB indicating lesser role of bottom tap root diameter on root branches. Interestingly, we did not observe any significant correlation between RA and other root traits in the current study. A lack of correlation between other traits and RA suggests that RA might be an independent trait which

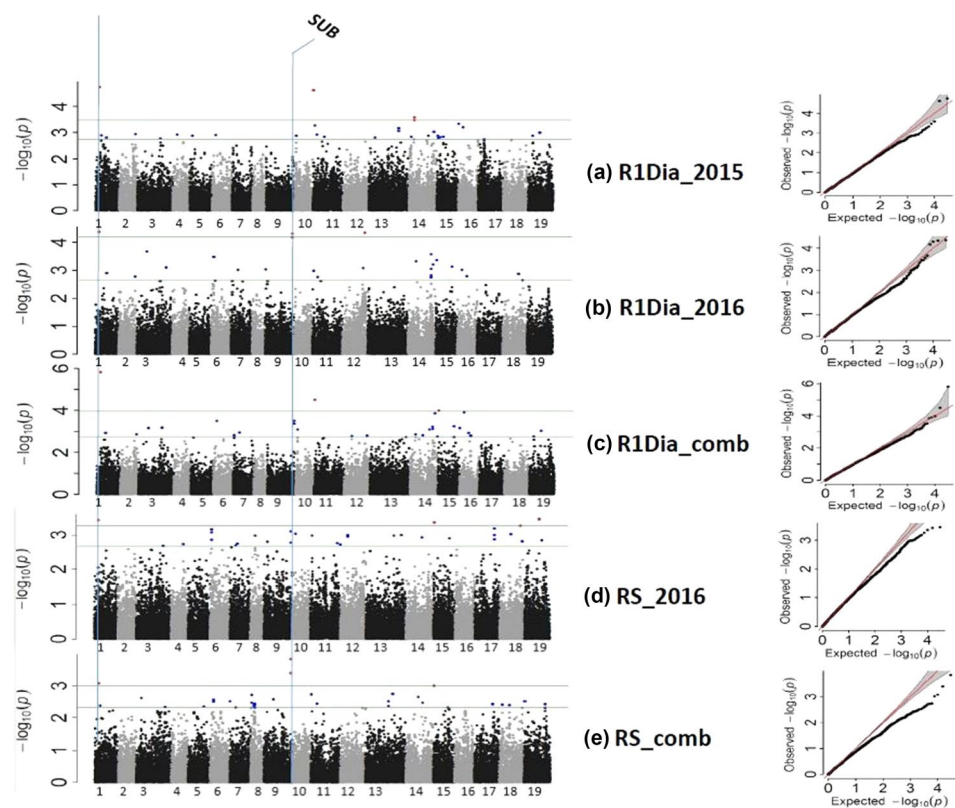
depends on soil environment rather than other root characteristics in *B. napus*.

Root diameters can be a proxy for other root traits

In the current study, multiple marker loci associated with R_1 Dia were also found to be associated with RS and PRB. Two marker loci on chromosome A01 (position about 2.04 Mbp) and chromosome C05 (position about 0.68 Mbp) were found to be associated with both R_1 Dia and RS and detected in multiple datasets (Fig. 6). Candidate gene *CYC2*; 3 and *PGP11* were identified close to the marker loci on chromosome C05 (position 0.68 Mbp). *CYC2* is involved in lateral root formation and triple *CYC2* mutant gives rise to defective lateral roots compared to the wild type (Vanneste et al. 2011). The *PGP* family of proteins consists of members of *ABC* transporter superfamily and few of them directly act as auxin efflux carrier in basipetal auxin transport and affect lateral root and root hair formation (Santelia et al. 2005). Two other significant marker loci, chrA09_32034411 and chrA09_32034416, are physically close and were found to be associated with RS and R_1 Dia, respectively (Fig. 6). Candidate gene *STRUBBELIG-receptor family 3 (SUB)* was found in the same region on chromosome A09. *SUB* is expressed in the root throughout the root development process and controls root meristem specification and epidermal root hair specification in *Arabidopsis* (Savage et al. 2013; Kwak and Schiefelbein 2014). Marker locus chrC01_rand_171065 was associated with PRB and R_1 Dia. In addition to these, two other marker loci on chromosome C05 are located within 9 kbp and are associated with both R_2 Dia and PRB. Candidate gene *Aminotransferase-like, plant mobile domain family protein* or *MAIN* or *MAINTENANCE OF MERISTEM* was found close to this marker locus. Experimental evidences suggest that mutants of *maintenance of meristem* have a defective stem cell niche in *Arabidopsis* roots (Wenig et al. 2013). *MAINTENANCE OF MERISTEM* homolog *MAIN-like 1* mutant has short primary root branches (Ühlken et al. 2014).

Common marker loci or a region associated with R_1 Dia, RS, PRB and R_2 Dia is expected because we took PRB data from the top 10 cm of the root system and RS scoring was based on visual appearance of the root system consisting of both PRB and taproot diameters. In our phenotypic study, R_1 Dia, PRB and RS were highly correlated with each other in both years. Higher soil level tap root diameter has higher root surface area to accommodate higher root lateral branches and root hairs. A root system with high tap root diameter is correlated with higher xylem area in cowpea (Burrige et al. 2017) which may transport water and nutrients from the root to the shoots more efficiently. A high phenotypic correlation between R_1 Dia and R_2 Dia also indicates that root diameters may have a positive role in defining root length. Burrige et al. (2017) suggested that taproot

Fig. 6 Manhattan plot and QQ plot showing the common significant markers associated with R1Dia and RS. **a** R1Dia_2015, **b** R1Dia_2016, **c** R1Dia_combine, **d** RS_2016 and **e** RS_combine



diameter at 10 cm may be related to the plants ability to explore a deeper soil horizon in drought conditions for cowpea. Considering all these aspects, we propose that tap root diameter in *B. napus* can be a good indicator for other root architectural traits and may serve as a proxy trait for the whole root system. Importantly, the soil level taproot diameter R_1 Dia can be measured without destroying the plant.

Significant marker loci associated with same trait in multiple datasets

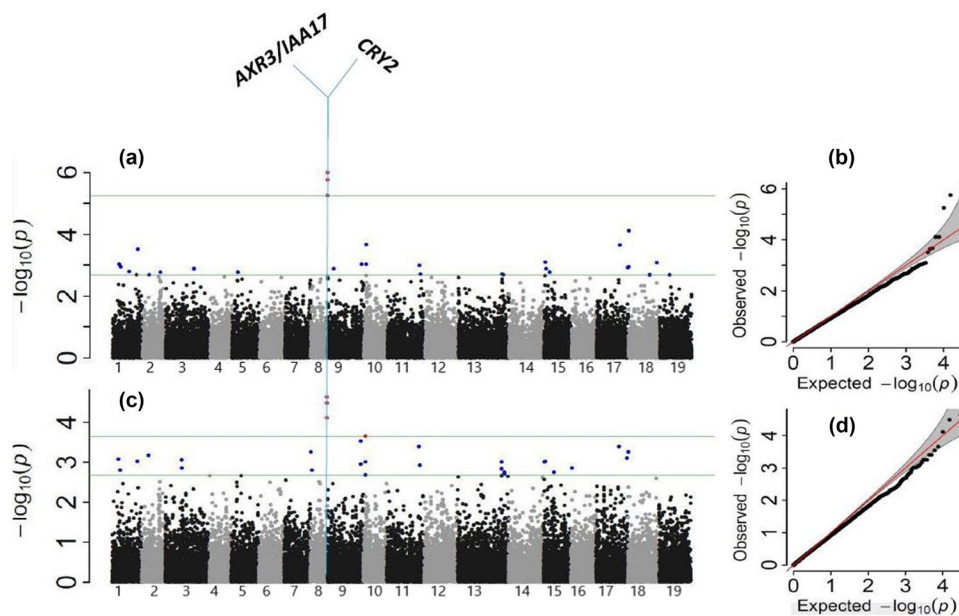
The marker locus chrA01_rand_2039614 was significantly associated with R_1 Dia in both 2015, 2016 and combined datasets. Marker locus chrC01_rand_171065 was also significantly associated with R_1 Dia in 2015 and the combined dataset. Marker locus chrC05_rand_678307 was identified in the combined dataset for R_1 Dia at 0.01 P value cutoff. However, with a less stringent 0.1 percentile P value cutoff, these marker loci were found to be significant in both 2015 and 2016. For R_2 Dia, three closely located marker loci on chromosome A08 (position about 18.4 Mbp) were found to be significantly associated in both 2015 and combined datasets. Two candidate genes, *AXR3* and *CRY2*, were detected in the same region of chromosome A08 (Fig. 7). *Auxin Resistant 3* or *AXR3/IAA17* overexpression caused defective roots in *Arabidopsis* (Kim et al. 2006). Knox (2003) reported that *AXR3/IAA17* inhibits root hair initiation and elongation. The

relative abundance of *AXR3/IAA17* and *SHY2/IAA3* (gene which induce root hair formation and elongation) in a cell is the determinant of root hair formation in *Arabidopsis*. Overexpression of *CRY2* in blue light results in reduced primary root elongation (Canamero et al. 2006).

For PRB, one marker locus chrC01_rand_171065 was repeatedly significant in 2015 and the combined dataset. Marker locus chrA06_2653673 was significantly associated with PRB in combined dataset was also detected in 2015 and 2016 at the less stringent 0.1 percentile P value cutoff. *Lateral Organ Boundary domain 1 (LBD1)* was detected close to this marker locus. Constitutive expression of *LBD1* in the *Medicago truncatula* root system subjected to salt stress regulates the overall root architecture (Ariel et al. 2010). Primary lateral roots appear from the taproot near the soil surface and are necessary for nutrient acquisition. Lateral roots in plants are highly responsive to the soil microenvironment. It has been reported that the length of lateral root was increased under low N condition in *Arabidopsis*, and lateral root density was increased in P-deficient soil conditions in rice (Desnos 2008; Gruber et al. 2013; Kong et al. 2014). Therefore, the significant markers identified for PRB in this study may be useful in future marker-assisted breeding program to select for improved nutrient acquisition.

Root angle is an important trait for root architecture where a narrower root angle allows the root to penetrate deeper into the soil horizon which reduces the competition between

Fig. 7 Manhattan plot and QQ plot showing the results of marker/trait association of R2Dia. **a** Manhattan plot of R2Dia in 2015, **b** QQ plot of R2Dia in 2015, **c** Manhattan plot of R2 in combined dataset, **d** QQ plot of R2 in combined dataset



the neighboring plants. In addition, the plant will have an excess of moisture from the deeper soil horizon too. Seven marker loci associated with root angle (RA) were identified in 2015, 2016 and the combined dataset. Among them, the marker locus chrA02_18466347 was found to be significant in both 2015 and the combined dataset. Root score was measured visually on the basis of overall appearances of the root system and eight marker loci were identified related to root score (RS). Marker locus chrA01_rand_2039614 was associated with RS in both 2016 and the combined datasets.

In summary, we followed the shovelomics approach to phenotype five root architectural traits and use the data for GWAS of these root traits with SNP markers. In this study, a total of 31 significant marker loci associated with different root traits were identified. Several marker loci were found to be associated with multiple root traits and appeared in multiple environments and potential for future marker-assisted selection for root traits in rapeseed/canola. It appears that tap root diameter in rapeseed/canola may be a determinant of the total root system in canola and can be a proxy trait for other root architectural traits. Tap root diameter at soil level (R₁Dia) can be measured without uprooting the plant from soil and, therefore, can potentially be a non-destructive measurement for root system characterization in rapeseed/canola. Fifteen candidate genes related to different root traits were detected within 100 kbp downstream and upstream of different significant markers.

Compliance with ethical standards

Conflict of interest The authors declare that they have no conflicts of interest.

Ethical approval The authors also declare that this article does not contain any studies related with human participants or animals performed by any of the authors and complies with ethical standard.

References

- Ariel FD, Diet A, Crespi M, Chan RL (2010) The *LOB*-like transcription factor *Mt LBD1* controls *Medicago truncatula* root architecture under salt stress. *Plant Signal Behav* 5:1666–1668. <https://doi.org/10.4161/psb.5.12.14020>
- Arifuzzaman M, Rahman M (2017) A comparative study on root traits of spring and winter canola (*Brassica napus* L.) under controlled and water stressed conditions. *J Agric Sci* 9:58. <https://doi.org/10.5539/jas.v9n7p58>
- Arifuzzaman M, Mamidi S, Mcclean P, Rahman M (2016) QTL mapping for root vigor and days to flowering in *Brassica napus* L. *Can J Plant Sci* 109:99–109. <https://doi.org/10.1139/cjps-2016-0048>
- Aulchenko YS, Ripke S, Isaacs A, van Duijn CM (2007) GenABEL: an R library for genome-wide association analysis. *Bioinformatics* 23:1294–1296. <https://doi.org/10.1093/bioinformatics/btm108>
- Begum H, Spindel JE, Lalusin A et al (2015) Genome-wide association mapping for yield and other agronomic traits in an elite breeding population of tropical rice (*Oryza sativa*). *PLoS ONE* 10:1–19. <https://doi.org/10.1371/journal.pone.0119873>
- Bucksch A, Burrige J, York LM et al (2014) Image-based high-throughput field phenotyping of crop roots. *Plant Physiol* 166:470–486. <https://doi.org/10.1104/pp.114.243519>
- Burrige J, Jochua CN, Bucksch A, Lynch JP (2016) Legume shovelomics: high-throughput phenotyping of common bean (*Phaseolus vulgaris* L.) and cowpea (*Vigna unguiculata* subsp. *unguiculata*) root architecture in the field. *Field Crop Res* 192:21–32. <https://doi.org/10.1016/j.fcr.2016.04.008>
- Burrige JD, Schneider HM, Huynh BL et al (2017) Genome-wide association mapping and agronomic impact of cowpea root architecture. *Theor Appl Genet* 130:419–431. <https://doi.org/10.1007/s00122-016-2823-y>
- Canamero RC, Bakrim N, Bouly JP et al (2006) Cryptochrome photoreceptors *cry1* and *cry2* antagonistically regulate primary root

- elongation in *Arabidopsis thaliana*. *Planta* 224:995–1003. <https://doi.org/10.1007/s00425-006-0280-6>
- Canè MA, Maccaferri M, Nazemi G et al (2014) Association mapping for root architectural traits in durum wheat seedlings as related to agronomic performance. *Mol Breed* 34:1629–1645. <https://doi.org/10.1007/s11032-014-0177-1>
- Clark RT, MacCurdy RB, Jung JK et al (2011) Three-dimensional root phenotyping with a novel imaging and software platform. *Plant Physiol* 156:455–465. <https://doi.org/10.1104/pp.110.169102>
- Colombi T, Kirchgessner N, Le Marie CA, et al (2015) Next generation shovelomics: set up a tent and REST. *Plant Soil*. <https://doi.org/10.1007/s11104-015-2379-7>
- Courtois B, Audebert A, Dardou A et al (2013) Genome-wide association mapping of root traits in a *Japonica* rice panel. *PLoS ONE* 8:1–18. <https://doi.org/10.1371/journal.pone.0078037>
- de Dorlodot S, Forster B, Pages L et al (2007) Root system architecture: opportunities and constraints for genetic improvement of crops. *Trends Plant Sci* 12:474–481. <https://doi.org/10.1016/j.tplants.2007.08.012>
- Desnos T (2008) Root branching responses to phosphate and nitrate. *Curr Opin Plant Biol* 11:82–87. <https://doi.org/10.1016/j.pbi.2007.10.003>
- Elias EM, Manthey FA (2016) Registration of “Joppa” durum wheat. *Crop Sci* 10:139–144. <https://doi.org/10.2135/cropsci2004.1025>
- Elshire RJ, Glaubitz JC, Sun Q, et al (2011) A robust, simple genotyping-by-sequencing (GBS) approach for high diversity species. *PLoS ONE*. <https://doi.org/10.1371/journal.pone.0019379>
- Ferreira ME, Satagopan J, Yandell BS et al (1995) Mapping loci controlling vernalization requirement and flowering time in *Brassica napus*. *Theor Appl Genet* 90:727–732. <https://doi.org/10.1007/BF00222140>
- Gong F, Wu X, Zhang H, et al (2015) Making better maize plants for sustainable grain production in a changing climate. *Front Plant Sci*. <https://doi.org/10.3389/fpls.2015.00835>
- Gruber BD, Giehl RFH, Friedel S, von Wiren N (2013) Plasticity of the *Arabidopsis* root system under nutrient deficiencies. *Plant Physiol* 163:161–179. <https://doi.org/10.1104/pp.113.218453>
- Hund A (2010) Genetic variation in the gravitropic response of maize roots to low temperatures. *Plant Root* 4:22–30. <https://doi.org/10.3117/plantroot.4.22>
- Kang HM, Zaitlen NA, Wade CM et al (2008) Efficient control of population structure in model organism association mapping. *Genetics* 178:1709–1723. <https://doi.org/10.1534/genetics.107.080101>
- Kebede B, Thiagarajah M, Zimmerli C, Rahman MH (2010) Improvement of open-pollinated spring rapeseed (*Brassica napus* L.) through introgression of genetic diversity from winter rapeseed. *Crop Sci* 50:1236–1243. <https://doi.org/10.2135/cropsci2009.06.0352>
- Kim H, Park PJ, Hwang HJ et al (2006) Brassinosteroid signals control expression of the *AXR3/IAA17* gene in the cross-talk point with Auxin in root development. *Biosci Biotechnol Biochem* 70:768–773. <https://doi.org/10.1271/bbb.70.768>
- Knox K (2003) *AXR3* and *SHY2* interact to regulate root hair development. *Development* 130:5769–5777. <https://doi.org/10.1242/dev.00659>
- Koboldt DC, Zhang Q, Larson DE et al (2012) VarScan 2: somatic mutation and copy number alteration discovery in cancer by exome sequencing. *Genome Res* 22:568–576
- Kong X, Zhang M, De Smet I, Ding Z (2014) Designer crops: optimal root system architecture for nutrient acquisition. *Trends Biotechnol* 32:597–598. <https://doi.org/10.1016/j.tibtech.2014.09.008>
- Kuijken RCP, Van Eeuwijk FA, Marcelis LFM, Bouwmeester HJ (2015) Root phenotyping: from component trait in the lab to breeding. *J Exp Bot* 66:5389–5401
- Kumar B, Abdel-Ghani AH, Reyes-Matamoros J et al (2012) Genotypic variation for root architecture traits in seedlings of maize (*Zea mays* L.) inbred lines. *Plant Breed* 131:465–478. <https://doi.org/10.1111/j.1439-0523.2012.01980.x>
- Kwak SH, Schiefelbein J (2014) *TRIPTYCHON*, not *CAPRICE*, participates in feedback regulation of SCM expression in the *Arabidopsis* root epidermis. *Plant Signal Behav*. <https://doi.org/10.4161/15592324.2014.973815>
- Li H (2013) Aligning sequence reads, clone sequences and assembly contigs with BWA-MEM. [arXiv:1303.3997](https://arxiv.org/abs/1303.3997) [q-bio.GN]
- Li X, Guo Z, Lv Y, et al (2017) Genetic control of the root system in rice under normal and drought stress conditions by genome-wide association study. *PLoS Genet*. <https://doi.org/10.1371/journal.pgen.1006889>
- Lin L, Allemekinders H, Dansby A et al (2013) Evidence of health benefits of canola oil. *Nutr Rev* 71:370–385. <https://doi.org/10.1111/nure.12033>
- Lipka AE, Tian F, Wang Q et al (2012) GAPIT: genome association and prediction integrated tool. *Bioinformatics* 28:2397–2399. <https://doi.org/10.1093/bioinformatics/bts444>
- Lou Q, Chen L, Mei H et al (2015) Quantitative trait locus mapping of deep rooting by linkage and association analysis in rice. *J Exp Bot* 66:4749–4757. <https://doi.org/10.1093/jxb/erv246>
- Luo X, Ma C, Yi B et al (2016) Genetic distance revealed by genomic single nucleotide polymorphisms and their relationships with harvest index heterotic traits in rapeseed (*Brassica napus* L.). *Euphytica* 209:41–47. <https://doi.org/10.1007/s10681-015-1629-3>
- Lynch JP (2007) Turner review no. 14. Roots of the second green revolution. *Aust J Bot* 55:493–512. <https://doi.org/10.1071/BT06118>
- Mamidi S, Chikara S, Goos RJ et al (2011) Genome-wide association analysis identifies candidate genes associated with iron deficiency chlorosis in soybean. *Plant Genome J* 4:154. <https://doi.org/10.3835/plantgenome2011.04.0011>
- Mamidi S, Lee RK, Goos JR, McClean PE (2014) Genome-wide association studies identifies seven major regions responsible for iron deficiency chlorosis in soybean (*Glycine max*). *PLoS ONE*. <https://doi.org/10.1371/journal.pone.0107469>
- Moghaddam SM, Mamidi S, Osorno JM, et al (2016) Genome-wide association study identifies candidate loci underlying agronomic traits in a Middle American diversity panel of common bean. *Plant Genome* 9:0. <https://doi.org/10.3835/plantgenome2016.02.0012>
- Pace J, Gardner C, Romay C, et al (2015) Genome-wide association analysis of seedling root development in maize (*Zea mays* L.). *BMC Genom*. <https://doi.org/10.1186/s12864-015-1226-9>
- Passioura JB (2012) Phenotyping for drought tolerance in grain crops: when is it useful to breeders? *Funct Plant Biol* 39:851–859. <https://doi.org/10.1071/FP12079>
- Price AL, Patterson NJ, Plenge RM et al (2006) Principal components analysis corrects for stratification in genome-wide association studies. *Nat Genet* 38:904–909. <https://doi.org/10.1038/ng1847>
- Rahaman M, Mamidi S, Rahman M (2017) Association mapping of agronomic traits of canola (*Brassica napus* L.) subject to heat stress under field conditions. *Aust J Crop Sci* 11:1094–1105. <https://doi.org/10.21475/ajcs.17.11.09.pne512>
- Rahman M, McClean P (2013) Genetic analysis on flowering time and root system in *Brassica napus* L. *Crop Sci* 53:141. <https://doi.org/10.2135/cropsci2012.02.0095>
- Santelia D, Vincenzetti V, Azzarello E et al (2005) *MDR*-like *ABC* transporter *AtPGP4* is involved in auxin-mediated lateral root and root hair development. *FEBS Lett* 579:5399–5406. <https://doi.org/10.1016/j.febslet.2005.08.061>
- Savage N, Yang TJW, Chen CY et al (2013) Positional signaling and expression of *ENHANCER OF TRY AND CPC1* are tuned to increase root hair density in response to phosphate deficiency in *Arabidopsis thaliana*. *PLoS ONE*. <https://doi.org/10.1371/journal.pone.0075452>
- Scheet P, Stephens M (2006) A fast and flexible statistical model for large-scale population genotype data: applications to inferring

- missing genotypes and haplotypic phase. *Am J Hum Genet* 78:629–644. <https://doi.org/10.1086/502802>
- Soltani A, Moghaddam S, Walter K et al (2017) Genetic architecture of flooding tolerance in the dry bean Middle-American diversity panel. *Front Plant Sci* 8:1–15. <https://doi.org/10.3389/fpls.2017.01183>
- Sun G, Zhu C, Kramer MH et al (2010) Variation explained in mixed-model association mapping. *Heredity (Edinb)* 105:333–340. <https://doi.org/10.1038/hdy.2010.11>
- Tabachnick B, Fidell L (2001) *Computer-assisted research design and analysis*. Allyn & Bacon, Boston, MA
- Thomas CL, Alcock TD, Graham NS et al (2016) Root morphology and seed and leaf ionic traits in a *Brassica napus* L. diversity panel show wide phenotypic variation and are characteristic of crop habit. *BMC Plant Biol* 16:1–18. <https://doi.org/10.1186/s12870-016-0902-5>
- Trachsel S, Kaeppeler SM, Brown KM, Lynch JP (2011) Shovelomics: high throughput phenotyping of maize (*Zea mays* L.) root architecture in the field. *Plant Soil* 341:75–87. <https://doi.org/10.1007/s11104-010-0623-8>
- Truong SK, McCormick RF, Rooney WL, Mullet JE (2015) Harnessing genetic variation in leaf angle to increase productivity of sorghum bicolor. *Genetics* 201:1229–1238. <https://doi.org/10.1534/genetics.115.178608>
- Ühlken C, Horvath B, Stadler R et al (2014) *MAIN-LIKE1* is a crucial factor for correct cell division and differentiation in *Arabidopsis thaliana*. *Plant J* 78:107–120. <https://doi.org/10.1111/tpj.12455>
- UN (1935) Genome analysis in *Brassica* with special reference to the experimental formation of *B. napus* and peculiar mode of fertilization. *Jpn J Bot* 7:389–452
- Vanneste S, Coppens F, Lee E et al (2011) Developmental regulation of *CYCA2s* contributes to tissue-specific proliferation in *Arabidopsis*. *EMBO J* 30:3430–3441. <https://doi.org/10.1038/emboj.2011.240>
- Vergauwen D, De Smet I (2017) From early farmers to Norman Borlaug—the making of modern wheat. *Curr Biol* 27:R858–R862
- Wang X, Chen Y, Thomas CL et al (2017) Genetic variants associated with the root system architecture of oilseed rape (*Brassica napus* L.) under contrasting phosphate supply. *DNA Res* 24:407–417. <https://doi.org/10.1093/dnares/dsx013>
- Wasson AP, Richards RA, Chatrath R et al (2012) Traits and selection strategies to improve root systems and water uptake in water-limited wheat crops. *J Exp Bot* 63:3485–3498. <https://doi.org/10.1093/jxb/ers111>
- Wenig U, Meyer S, Stadler R et al (2013) Identification of *MAIN*, a factor involved in genome stability in the meristems of *Arabidopsis thaliana*. *Plant J* 75:469–483. <https://doi.org/10.1111/tpj.12215>
- York LM, Lynch JP (2015) Intensive field phenotyping of maize (*Zea mays* L.) root crowns identifies phenes and phene integration associated with plant growth and nitrogen acquisition. *J Exp Bot* 66:5493–5505. <https://doi.org/10.1093/jxb/erv241>
- Zhang Y, Thomas CL, Xiang J et al (2016) QTL meta-analysis of root traits in *Brassica napus* under contrasting phosphorus supply in two growth systems. *Sci Rep* 6:1–12. <https://doi.org/10.1038/srep33113>
- Zhao JH (2007) Gap: genetic analysis package. *J Stat Softw* 23:1–18. <https://doi.org/10.18637/jss.v023.i08>
- Zhao Y, Wang H, Chen W, Li Y (2014) Genetic structure, linkage disequilibrium and association mapping of verticillium wilt resistance in elite cotton (*Gossypium hirsutum* L.) germplasm population. *PLoS ONE*. <https://doi.org/10.1371/journal.pone.0086308>
- Zhu J, Ingram PA, Benfey PN, Elich T (2011) From lab to field, new approaches to phenotyping root system architecture. *Curr Opin Plant Biol* 14:310–317. <https://doi.org/10.1016/j.pbi.2011.03.020>

Publisher's Note Springer Nature remains neutral with regard to jurisdictional claims in published maps and institutional affiliations.